Physiological and Molecular Plant Pathology (2002) **61**, 109–120
doi:10.1006/pmpp.2002.0419, available online at http://www.idealibrary.com on IDEAL®

Ultrastructural changes and immunocytochemical localization of the elicitin quercinin in *Quercus robur* L. roots infected with *Phytophthora quercina*

M. BRUMMER, M. AREND, J. FROMM, A. SCHLENZIG and W. F. OßWALD*

[1]*Department of Ecology, Section Forest Phytopathology, Technische Universität München, Am Hochanger 13, 85354 Freising, Germany and* [2]*Department of Wood Biology, Technische Universität München, Winzererstr. 45, 80797 München, Germany*

(Accepted for publication 27 June 2002)

We report on the growth pattern of the root rot pathogen *Phytophthora quercina* in roots of oak seedlings and on the localization of its elicitin quercinin. Some hours after infection, the pathogen was mainly found in the intercellular spaces of the cortical parenchyma. Some parenchyma cells were also invaded by *P. quercina* and the plasmalemma of those cells as well as of neighbouring cells separated from the cell wall. Transmission electron microscopy studies proved that *P. quercina* penetrated the cell walls forming haustorial-like structures in invaded cells. These structures and cell wall appositions were covered with electron dense material.

Immunofluorescence investigations in combination with a specific anti cryptogein antibody clearly showed that the *P. quercina* elicitin quercinin was located within the hyphal cell wall and seems to be released into invaded cells. In addition, immunogold labelling showed that quercinin was found in the intercellular spaces as well as in penetrated cells. Finally, we demonstrated with ELISA that quercinin was produced by the pathogen in infected tissue during the whole growth phase.

Keywords: *Phytophthora quercina*; oak; elicitin; quercinin; immunogold labelling; immunofluorescence detection; ultrastructure; transmission electron microscopy.

INTRODUCTION

Phytophthora species attack numerous economically important crop and woody plants [*11*]. Recently Jung *et al*. [*18*, *19*] and Cooke *et al*. [*6*] identified *Phytophthora quercina* as a new species that is strongly involved in oak decline on sites with a mean soil pH above 3·5 and sandy-loamy to clayey soil texture. Isolations from fine roots and rhizosphere soil samples demonstrated the widespread occurrence of Phytophthora species including *P. quercina* all over Europe [*13*, *18*]. Soil infection tests showed that *P. quercina* and *P. cambivora* were the most aggressive species towards roots of young oak (*Quercus robur* L.) plants [*17*].

The symptoms of plants infected with different Phytophthoras include leaf discoloration and severe wilting of leaves. Several investigations on physiological parameters demonstrate that photosynthesis, transpiration and hydraulic conductivity are significantly reduced after infection by Phytophthora [*8*, *24*, *27*]. The authors concluded that the weak physiological activity observed in the leaves of infected plants could be due to the loss of fine roots, plugging of xylem pit membranes by tyloses, Phytophthora mediated hormonal imbalance or to toxins released by the root pathogen.

Recently Heiser *et al*. [*14*] have proven that *P. quercina* released the elicitin quercinin in liquid culture, as has been shown for numerous other Phytophthora species [*35*, *37*]. The molecular weight of quercinin of about 10 kDa [*14*] is similar to the molecular weights of other elicitins [*21*]. Kamoun *et al*. [*21*] investigated 52 Phytophthora isolates representing 13 species which were shown to produce 10 kDa elicitins. On the basis of their amino acid sequences, their isoelectric points and their effects on tobacco plants, elicitins are grouped into two classes. The α-elicitins contain a valyl residue at position 13 and exhibit an acidic isoelectric point, whereas basic β-elicitins carry lysine at position 13. *P. quercina* was shown to produce elicitins with both acidic and basic isoelectric points [*14*]. It was demonstrated that quercinin showed a high homology to cryptogein as it was picked up by antibodies to cryptogein, the elicitin of *P. cryptogea* on Western blots [*14*]. Knowing this fact, we could use anti cryptogein antibodies for the immunolocalization of quercinin in infected oak root tissue.

* To whom all correspondence should be addressed. E-mail: osswald@bot.forst.tu-muenchen.de

0885-5765/02/$ - see front matter

When taken up by tobacco leaves, quercinin elicited wilting, chlorosis and necrosis [*14*] similar to the observations of Csinos and Hendrix [*7*] on tobacco leaves treated with cryptogein. Wendehenne *et al*. [*33*] proved that specific binding sites for cryptogein, the elicitin of *P. cryptogea*, are localized within tobacco plasma membranes. Tavernier *et al*. [*28*] and Pugin and Guern [*25*] showed that early events induced by cryptogein in tobacco cells are the stimulation of a plasma membrane NADPH oxidase generating superoxide and the activation of glycolysis and the pentose phosphate pathway, which generate NADPH. Cryptogein has also been shown to catalyse the transfer of sterols between phospholipidic membranes [*23*]. Thus, elicitins could act as sterol carrier proteins and transfer sterols from plant plasma membranes to the hyphae.

The aim of our investigations was to get information on the growth of *P. quercina* in infected oak roots and to localize the peptide quercinin in roots using immunocytochemical techniques.

MATERIALS AND METHODS

Plant material and infection of roots with zoospores for microscopic investigations

For all microscopic investigations, 4 week old seedlings of *Q. robur* L. were used. *P. quercina* isolate Hag4/2 was isolated from rhizosphere soil of diseased oaks in the field [*19*]. The isolate was further cultivated on V8-Agar at 18 °C. Before use, small pieces of mycelium of a V8-Agar culture were transferred to new V8-Agar plates and incubated at 18 °C for 5 days. For the inoculation of V8-liquid cultures small pieces of mycelium of the outer part of these cultures were used. Erlenmeier flasks with freshly prepared and autoclaved V8-medium were inoculated with five pieces of mycelium each and incubated for about 1 week at 18 °C. The obtained mycelium cultures were washed in distilled water and incubated in filter-sterilized oak root exudate for 6–8 days at 18 °C to stimulate the formation of zoosporangia. The root exudate had been obtained by incubation of oak saplings in water for 3 days at room temperature. The zoospores were released by the zoosporangia after incubation at 4 °C for 1 h in the dark and 24 °C for 1/4 h under illumination. The zoospore suspension was filtrated through four layers of mull under sterile conditions. The density of zoospores was estimated with a Sedwick Rafter S50 and adjusted to a concentration of 10 zoospores ml^{-1} with autoclaved water. Oak roots were infected by incubating the root tips in the zoospore suspension for 5–7 days at 20 °C. Roots of control plants were kept in autoclaved water. For microscopic investigations small root segments were cut with a razor blade about 1–1·5 cm above the root tips. Thus, we obtained one root segment per root. For light microscope investigations, we used the tap roots of four infected plants and of four healthy control plants, respectively. For immunocytochemical investigations we used four root samples as uninfected controls, four as infected but unspecifically treated controls and four as infected specifically labelled samples. Of each root sample 5–10 sections were examined. In total we examined 20–40 sections per treatment. For immunogold-labelling experiments, mycelium of *P. quercina* was obtained from isolates growing on V8-Agar. Four samples of mycelium of one V8-Agar disk were treated specifically and four samples of the same disk unspecifically. Of each sample 5–10 sections were studied. Again we examined 20–40 sections of each treatment in total.

Preparation of root tissue for light microscopy

Root tissue was fixed with 3 % formaldehyde in Phosphate Buffer Saline (PBS) for 2 h, washed in buffer and dehydrated in graded series of ethanol. After embedding in LR White acryl resin, semi-thin sections were cut with a diamond knife and stained with 0·05 % aqueous solution of toluidine blue for light microscopy.

Preparation of root tissue for transmission electron microscopy

Root tissue was fixed with 6 % glutaraldehyde in 50 mM sodium cacodylate (pH 7·0) for 2 h, rinsed in buffer and post-fixed with 2 % osmium tetroxide at 4 °C overnight. After washing in buffer and in distilled water, the samples were stained with 1 % uranyl acetate in 20 % ethanol for 15 min, dehydrated in graded series of ethanol and embedded in Spurr's epoxy resin [*26*]. Ultrathin sections, cut with a diamond knife, were transferred onto formvar coated copper grids and stained with lead citrate. Sections were examined in a Zeiss EM 10c transmission electron microscope at 80 kV.

Immunolabelling for fluorescence microscopy

Root segments were fixed with 3 % formaldehyde (freshly prepared from paraformaldehyde) in PBS (pH 7·2) for 45 min. After washing in buffer, cross sections of 60 μm were made with a microtome and rinsed in buffer. To reduce unspecific labelling, sections were blocked with 100 mM glycine and 5 % goat normal serum, 1 % bovine serum albumin (BSA, fraction V) both in Phosphate Buffer Saline with 0·2 % Tween 20 (PBS-T) for 30 min. For immunolocalization, sections were incubated with anti-cryptogein rabbit serum diluted 1:500 in PBS containing 0·5 % BSA for 2 h at 37 °C. Incubation of non-infected roots with anti-cryptogein rabbit serum

served as control. As a further control, infected roots were incubated with preimmune rabbit IgG diluted 1:250. Following washing in PBS-T and PBS the sections were incubated with Cy3 labelled goat anti rabbit antibody diluted 1:200 in PBS containing 0·5 % BSA for 1 h at 37 °C. After washing in PBS-T and PBS the sections were viewed using a Zeiss axiophot microscope with filter combination 546 nm exciter, 575 nm dichroic, 590 nm emitter or with the laser scanning microscope (Zeiss LSM 5) under a wavelength of 543 nm.

Immunolabelling for transmission electron microscopy

Root segments or pieces of mycelium of *P. quercina* grown on V8-Agar were pre-fixed with 3 % formaldehyde (freshly prepared from paraformaldehyde) in PBS (pH 7·2). After 30 min the surfaces of the root segments or mycelium samples were cut again with a very sharp razor blade to open the first slightly fixed cell layer. Then the segments were incubated in the same formaldehyde solution once more for 30 min. Thus we obtained a slightly fixed surface on each of our segments, the interior of cells lying open. In this way, the aqueous solutions used in the following procedure had access to apoplasts as well as to the protoplasts of the first cell layer. All samples were rinsed in PBS-T and unspecific binding sites were blocked as described above. For immunolocalization, samples were incubated with anti-cryptogein rabbit serum diluted 1:500 in PBS containing 0·5 % BSA at 4 °C overnight. Samples from non-infected roots incubated with anti-cryptogein rabbit serum and infected roots incubated with preimmune rabbit IgG diluted 1:250 served as controls. Likewise control samples of mycelium were incubated with preimmune rabbit IgG diluted 1:250. Following washing in PBS-T and PBS, the samples were incubated with gold-labelled goat anti rabbit antibody (1 nm gold labelled; British BioCell, U.K.) diluted 1:400 in PBS containing 0·5 % BSA for 1 h at 37 °C. We used small 1 nm gold labelled secondary antibodies because these small particles were assumed to have a better access to the root tissue than usually used larger gold conjugates. After washing in PBS-T and PBS, the samples were post-fixed with 2 % glutaraldehyde in PBS for 30 min and washed in distilled water. For visualizing the 1 nm gold particles at the electron microscope level, silver enhancement was carried out with a silver enhancing kit (British BioCell, U.K.) according to the manufacturer's instructions. Samples were thereafter dehydrated and embedded in Spurr's epoxy resin [*26*]. The preparation of the embedded root samples for the ultramicrotome (LKB) was performed without damage to the sample surfaces. Thus ultrathin sections, cut with a diamond knife on the ultramicrotome, were taken from the outside tissue-layer. As one could assume a cell diameter of about 20 μm and sections of 0·01 μm were prepared, we obtained enough sections for our investigations of the first cell layer lying open on the surface of the root segments. The sections were transferred onto Formvar coated copper grids, and stained with lead citrate. Sections were examined in a Zeiss EM 10 transmission electron microscope at 80 kV.

Quantification of hyphal growth and of quercinin using ELISA-techniques

Four week old oak seedlings with tap-roots of about 10 cm length were infected with zoospores of *P. quercina* isolate Hag4/2 by incubating the root tips in a zoospore suspension (10 zoospores ml^{-1}) for 1–5 days at 20 °C. The whole fine root system (diameter 0–2 mm) was harvested from each plant 1–5 days after infection. Samples were frozen in liquid nitrogen, freeze dried and ground to powder. Five mg of each sample were extracted with 1 ml of the extraction buffer (50 mM carbonate buffer pH 9·6) for 20 min on ice. Afterwards, the extract was centrifuged at 13 000 ***g*** for 5 min. One hundred μl of a 1:100 dilution of each supernatant were used for the enzyme immunoassay. *P. quercina* infection was quantified using the Agri-Screen-Phytophthora detection Kit from Adgen (Agrifood diagnostic, Scotland) following the instructions of the manufacturer. The peptide quercinin was detected with specific antibodies from rabbit raised against cryptogein in combination with secondary anti rabbit antibodies from goat conjugated with alkaline phosphatase. 4-nitrophenyl phosphate disodium salt (Sigma 104 phosphate substrate) was used as substrate. The absorbance was measured by an ELISA reader at 405 nm.

RESULTS

Light microscopy

Fig. 1 shows healthy control roots of *Quercus robur* L. (a) and roots infected with *P. quercina* (b) 5 days after inoculation. Inter- and intra-cellular growing hyphae could be found within the rhizodermis and cortical parenchyma of all studied root sections. The plasmalemma of some cells was separating from the cell wall (*), indicating severe loss of cell turgor. This observation was made in all studied root sections. The percentage of cells showing plasmolysis ranged from 5 to 80 % depending on the intensity of infection. Compared to healthy tissue [Fig. 1(a)], a thickening of cell walls could be observed in infected tissue of about 50 % of all sections [Fig. 1(b)]. Even the endodermis, which forms a close-fitting cylinder in healthy roots, was destroyed by the pathogen in all studied root sections. In about 5 % of all studied root sections some hyphae were also found within xylem vessels (data not shown).

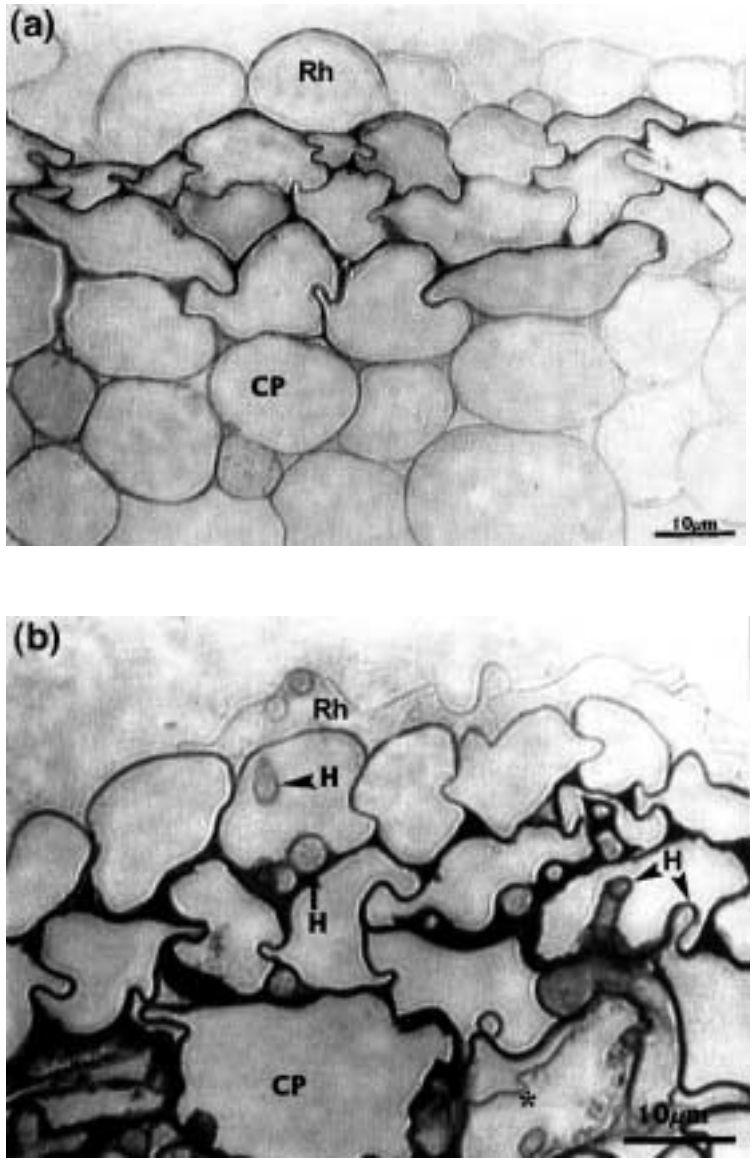

FIG. 1. Light microscopic studies of healthy and diseased oak roots infected with *P. quercina* 5 days after inoculation. (a) Cross section of a healthy control root showing the rhizodermis (Rh) and parts of the cortical parenchyma (CP). Bar = 10 μm. (b) Cross section of an infected root demonstrating the growth of hyphae (H) of *P. quercina*. *, plasmalemma separating from the cell wall. Bar = 10 μm.

Transmission electron microscopy

Fig. 2(a) shows an intercellular growing hypha contacting a neighbouring host cell which reacted to this stimulus by building a cell wall apposition at the opposite site. This observation was made in about 10 % of cells infected with the pathogen. Several vesicles were visible within all penetrating hyphae, as it is shown in Fig. 2(b). Electron-dense material (EdM) was deposited on to the cell wall, which also covered the haustorial-like structures [Fig. 2(b) and (c)]. This observation was made in all studied sections and in about 90 % of all penetrating hyphae. The electron dense material was first visible where the hypha was contacting the host cell wall [Fig. 2(a)] and seemed to be deposited on cell wall appositions mainly formed close to the penetration site [Fig. 2(d)].

Immunofluorescence labelling

Infected oak root samples were first incubated with the primary anti-cryptogein antibody specific for quercinin and finally with the Cy 3 labelled secondary antibody to get information on the location of quercinin within infected tissues. It turned out that quercinin was found

within the cell walls of hyphae growing in the intercellular space of the cortical parenchyma [Fig. 3(a)]. We detected numerous fluorescing hyphae in all studied sections of specifically marked infected root sections. Due to the rather strong autofluorescence of the stele region, specific fluorescence of hyphae could not be identified in this area (data not shown).

Using a confocal laser scanning microscope, a more detailed view was achieved. Again, only the hyphal cell wall of *P. quercina* growing in the intercellular spaces of the cortical parenchyma was highlighted [Fig. 3(b)]. One could get the impression that the pathogen released its quercinin into the penetrated cell (white arrow). This observation was made in three out of four experiments when cross sections of infected root tissue were analysed. Uninfected control tissue incubated with the specific primary antibody in combination with the Cy 3 labelled secondary antibody and infected tissue treated with

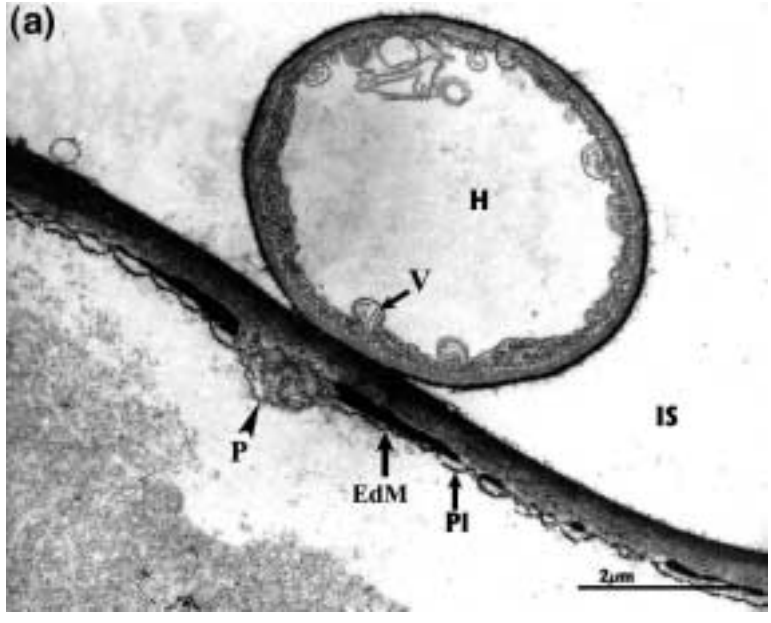

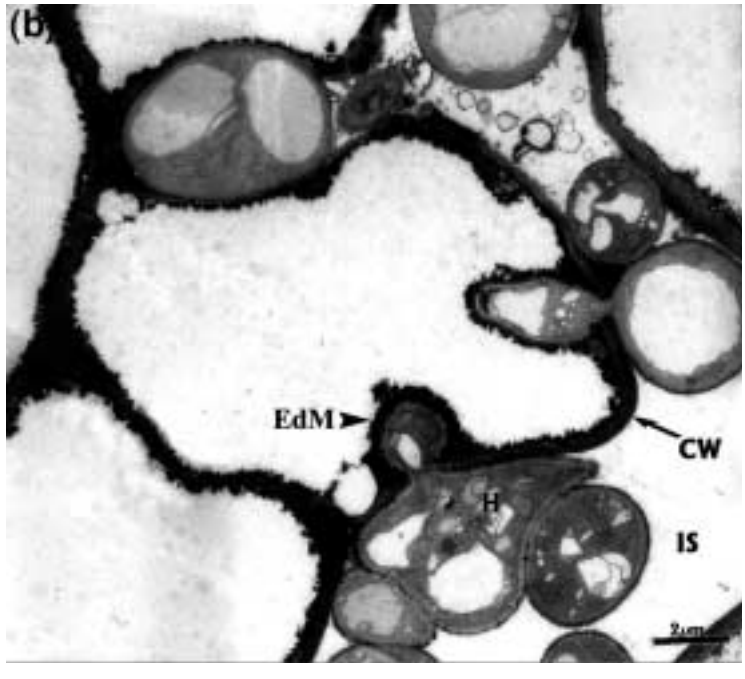

FIG. 2. continued over page.

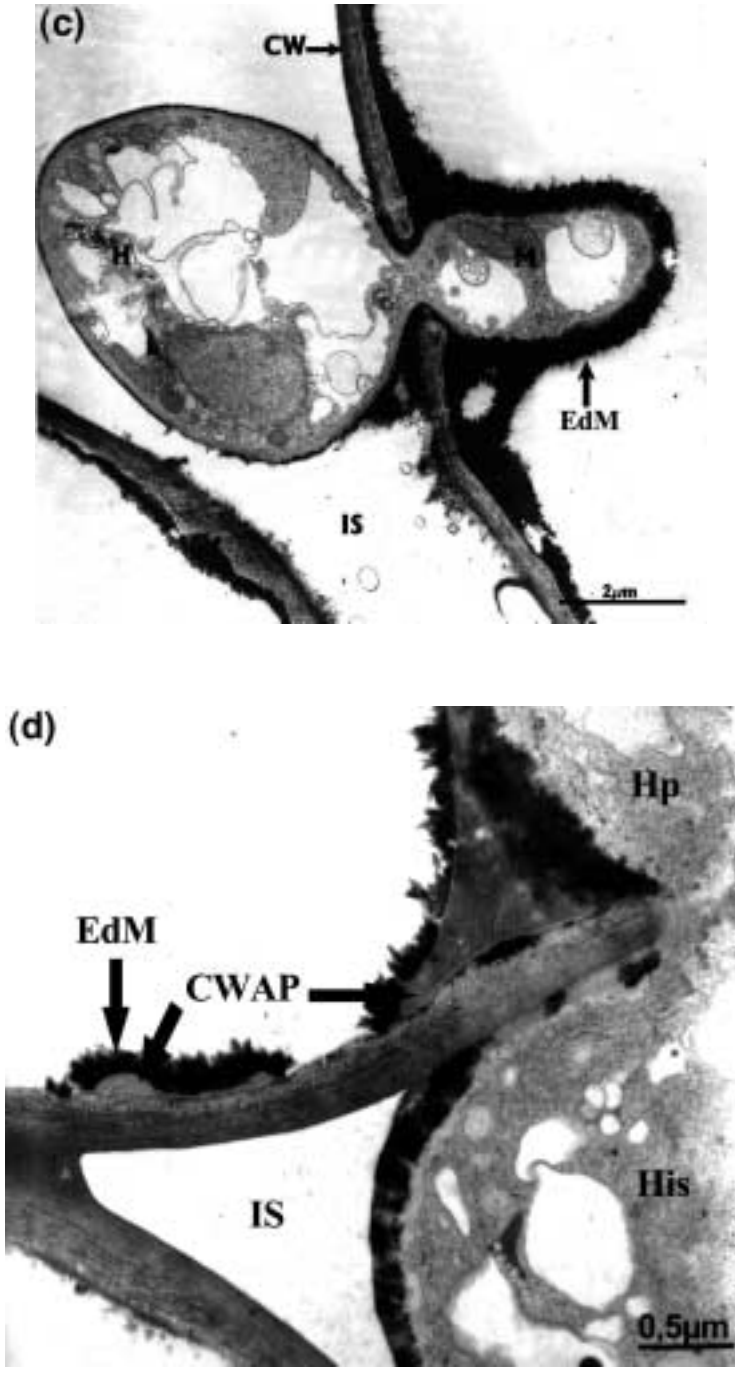

FIG. 2. Transmission electron microscopic photographs of an oak root infected with *P. quercina* 5 days after inoculation. (a) An intercellular growing hypha (H) with vesicles (V) inside touches the cell wall of a plant cell in the cortical parenchyma. Where the hypha gets in contact with the cell wall, papilla formation (P) is observed. An electron dense material (EdM) is deposited between the cell wall and the plasmalemma (Pl). Bar = 2 μm. (b) Hyphae growing in the intercellular space (IS) are invading a plant cell of the cortical parenchyma by penetrating the host cell wall (CW). Electron-dense material (EdM) is deposited. Bar = 2 μm. (c) Detailed view of a hypha invading a plant cell of the cortical parenchyma with a layer of electron-dense material (EdM) covering the haustorium-like structure. Mitochondria (M) are visible in the haustorial-like structure. Bar = 2 μm. (d) Detailed view of a hypha, growing in the intercellular space (IS), penetrating a host cell. Cell wall appositions (CWAP) are visible on which electron-dense material (EdM) is deposited. Bar = 0·5 μm. His = hypha within the intercellular space; Hp = hypha penetrating the host cell.

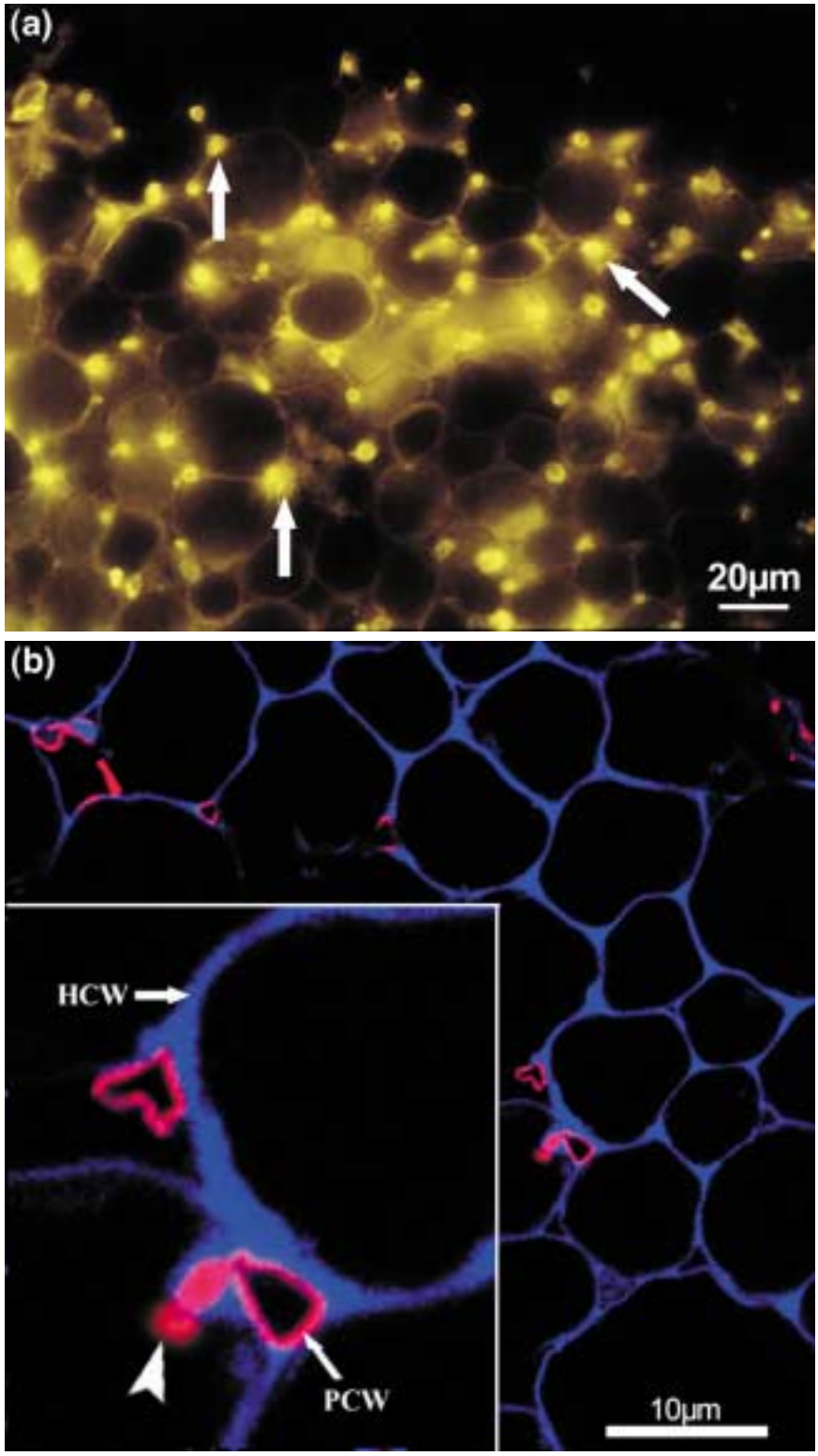

FIG. 3. Immunofluorescence investigations of roots infected with *P. quercina* in order to localize the *P. quercina* peptide quercinin 5–7 days after inoculation. The yellow fluorescence at a wavelength of 543 nm in (a) is due to the Cy3-marked secondary antibodies localizing quercinin. In (b) this colour was changed by the software hooked up to the laser scanning microscope into red. The blue colour shows the autofluorescence of the plant cell walls at the wavelength of 633 nm. Both pictures were superimposed to generate (b). (a) Only hyphae, mainly growing in the intercellular space are highlighted (white arrows). Bar = 20 μm. (b) Detailed view of the cortical parenchyma infected with *P. quercina* using laser scanning microscopy. Only cell wall structures of *P. quercina* (PCW) growing in the intercellular space are clearly highlighted. The peptide quercinin might be released into the host cell at the tip of the penetrating hypha (white arrow). HCW = host cell wall. Bar = 10 μm.

preimmune serum together with the same secondary antibody did not show such specific fluorescence in the cortical parenchyma (data not shown).

Immunofluorescence experiments were repeated four times showing exactly the same picture as presented in Fig. 3(a) and (b).

Immunogold labelling

In parallel to the immunofluorescence investigations, samples were prepared for the transmission electron microscope. In infected roots treated with anti-cryptogein serum, quercinin could be localized with gold-conjugated secondary antibodies. Silver enhanced gold particles were attached to about 70 % of the cell wall structures of hyphae which were found in the intercellular space [Fig. 4(c)]. Some gold particles were also observed on the outside of the host cell wall adjacent to the intercellular growing hyphae. Strong labelling was also found on the outside of the hyphae growing within host cells of the cortical parenchyma [Fig. 4(d)] and within infected protoxylem vessels [Fig. 4(e)]. We obtained these results by about 80 % of our studied root sections. Infected tissue treated with pre-immune rabbit serum in combination with gold-conjugated secondary antibody did not give such a specific distribution of gold particles [Fig. 4(b)]. Uninfected control root tissue treated with primary and secondary antibodies did not show any gold particles [Fig. 4(a)]. All cells were fully turgid. The structures of the cytoplasm, cell organelles and nuclei were clearly visible.

As we wanted a further support for our results, we investigated mycelium of *P. quercina* cultivated on V8-Agar and prepared it for the electron microscope. Again silver enhanced gold labelled particles were seen along the hyphal cell walls [Fig. 5(a)]. This observation was made in all sections and at least of 90 % of all investigated hyphae. Mycelium incubated in control solution containing preimmune rabbit serum did not give such a specific labelling [Fig. 5(b)].

Quantification of hyphal growth and of the peptide quercinin

In order to get information on hyphal growth and on quercinin synthesis in infected roots, both were quantified

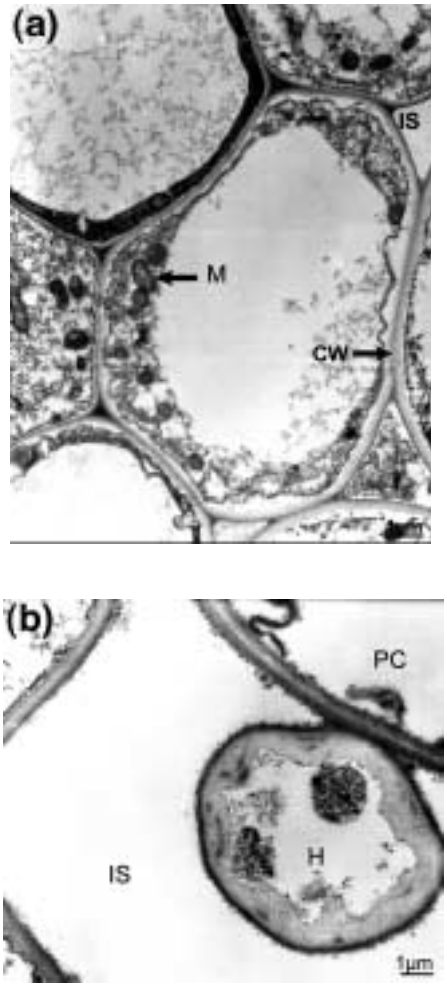

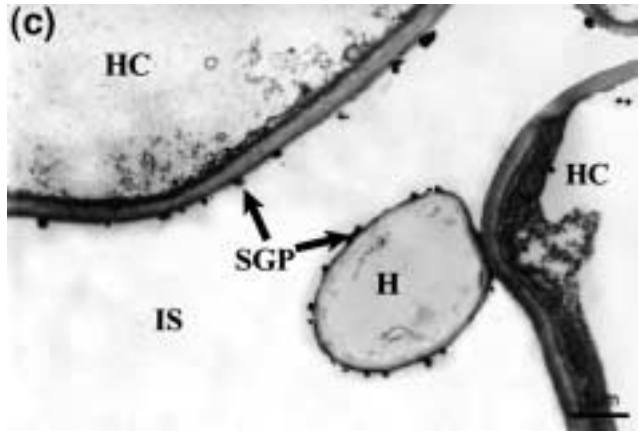

FIG. 4. Transmission electron microscopy in combination with silver enhanced immunogold labelling in order to localize the *P. quercina* peptide quercinin in infected oak roots 5 days after inoculation. (a) Cross section of cortical parenchyma of a healthy, not infected oak root. Turgescent cells with mitochondria (M) and small intercellular spaces (IS) can be seen. This tissue was treated with specific primary and secondary antibody as it was done for the cross sections in (c–e). Bar = 1 μm. (b) Cross section of a hypha (H) of *P. quercina* growing in the intercellular space (IS) of infected cortical parenchyma tissue. This tissue has been incubated with preimmune serum in combination with the secondary antibody conjugated with 1 nm gold particles. Bar = 1 μm. (c) Intercellular-growing hypha in the cortical parenchyma. This tissue has been treated with primary and secondary antibodies. Silver enhanced gold particles (SGP) are found on the outside of the hypha (H) and on the outside of the cell wall of an adjacent host cell (HC). Bar = 1 μm.

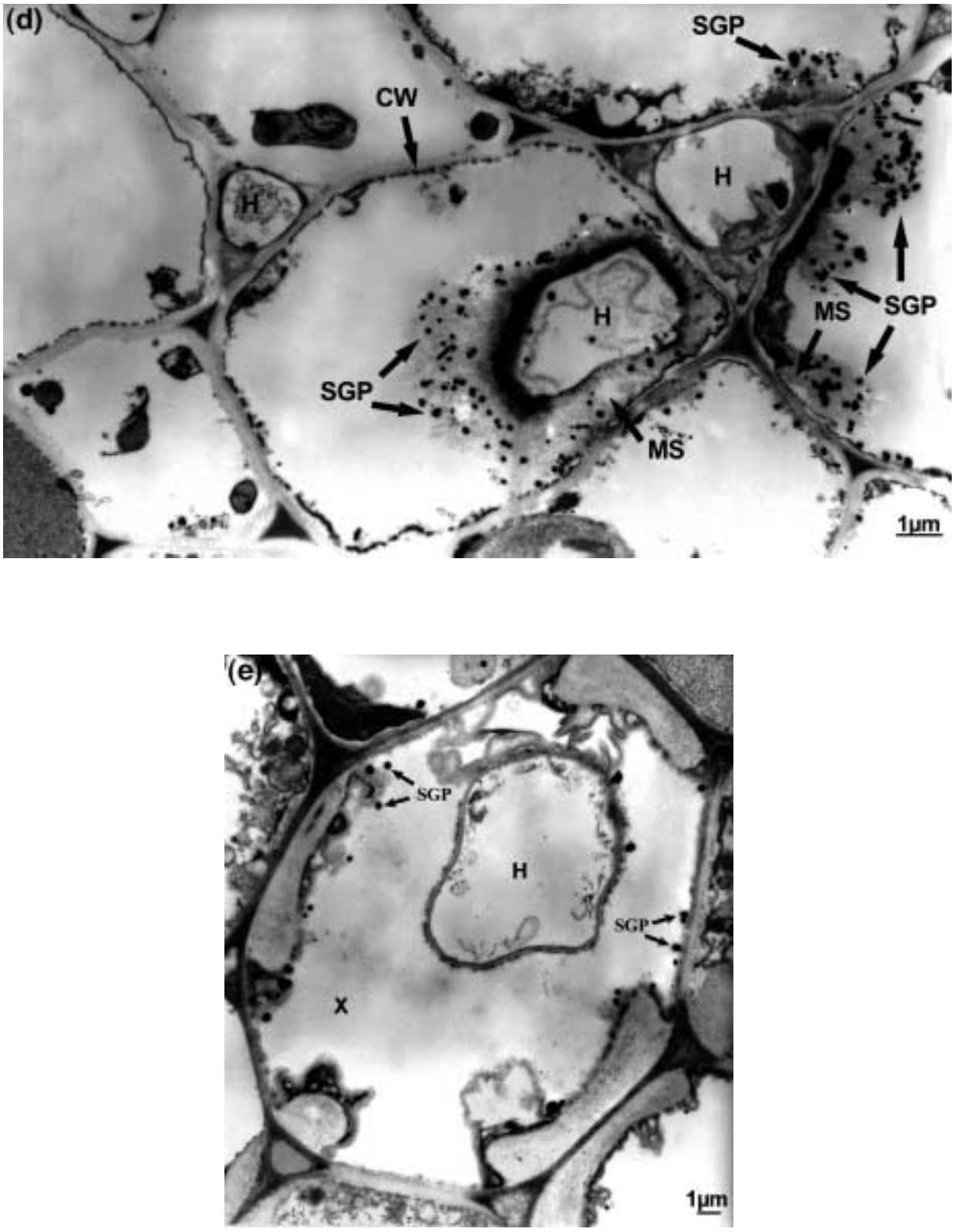

FIG. 4. (d) Massive accumulation of silver enhanced gold particles (SGP) is also found around hyphae (H) within invaded cells, mainly embedded in a matrix structure (MS). Bar = 1 μm. This tissue was treated with primary and secondary antibodies. (e) Localization of silver enhanced gold particles (SGP) in protoxylem vessels (X) invaded by a hypha (H) of *P. quercina*. Bar = 1 μm. This tissue was also treated with primary and secondary antibodies.

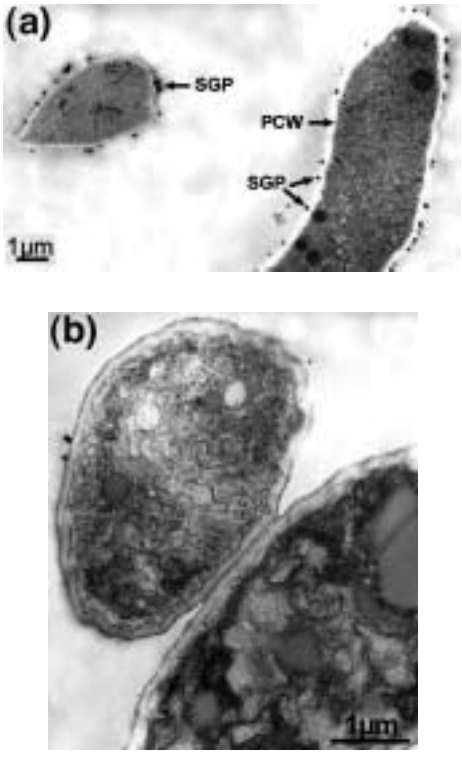

FIG. 5. Detection of quercinin in mycelium of *P. quercina* (V8-agar culture) by silver enhanced immunogold labelling. (a) Silver enhanced gold particles (SGP) are seen all over the outer hyphal cell wall (PCW). Bar = 1 μm. (b) Cross section of *P. quercina* hyphae incubated with preimmune serum in combination with gold conjugated secondary antibody. Bar = 1 μm.

using ELISA techniques. Fig. 6 shows that the patterns for hyphal growth and for peptide synthesis were comparable, proving that quercinin was released into the tissue during the whole growth phase of the root pathogen.

DISCUSSION

The aim of our investigations was to get information on the growth of *P. quercina* in infected oak roots and to localize the elicitin quercinin. In our pathosystem, *P. quercina* formed inter- and intra-cellular growing hyphae in the cortical parenchyma [Figs 1(b) and 2(b)]. The mode of penetration of root tissue by *P. quercina* conforms with observations of other root pathogenic Phytophthora species [*34*]. As demonstrated in Figs 1(b), 2(b) and (c), the middle lamellae were destroyed by intercellular growing hyphae. In hyphae penetrating into host cells the accumulation of hyphal cytoplasm became obvious [Fig. 2(b) and (c)]. Vesicles merging with the hyphal plasmalemma were present in these regions. Similar observations are reported by Børja *et al.* [*2*] for *Picea abies* infected with *Pythium dimorphum*.

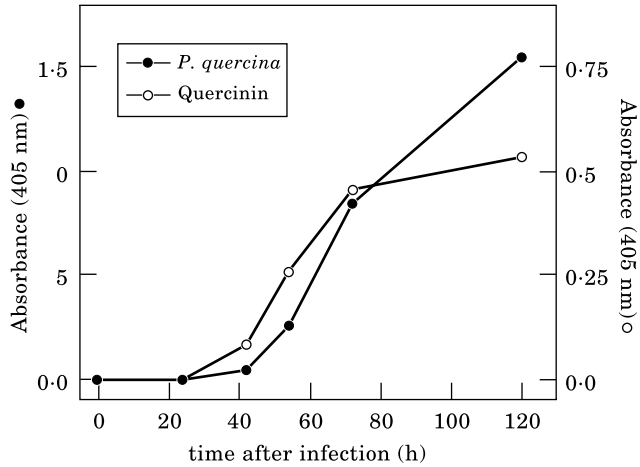

FIG. 6. Simultaneous quantification of *P. quercina* and of the peptide quercinin in infected root tissue using ELISA. The root rot pathogen *P. quercina* was quantified with the Phytophthora Kit (Adgen) and quercinin with the anti-cryptogein rabbit serum with ELISA techniques in infected fine root samples over a time period of 120 h as mentioned in Materials and Methods.

By cytological means, it could not be decided, whether the host cell walls were mechanically disrupted or enzymatically dissolved. Nevertheless, as no obvious disruption of cell walls at the point of penetration of hyphae of *P. quercina* into oak root cells could be observed, it seems likely [*1*], that extracellular enzymes of Phytophthora might be involved.

In many cases, we observed the shrinkage of the protoplasm which led to the separation of the plasmalemma from the plant cell wall. An example is shown in Fig. 1(b) (asterisk). Finally, the cortical host cells collapsed in the vicinity of hyphae [Fig. 1(b)]. There are numerous investigations on the interaction of other woody plants with several Phytophthora-species supporting our results [*3*, *12*, *16*, *29*, *34*].

Transmission electron microscopic investigations showed that electron-dense material was deposited around penetrating hyphae [Fig. 2(c)]. This could be interpreted as the formation of an extrahaustorial matrix. However, this electron dense material was found closely attached to cell wall appositions in the whole cell even far away from the penetration site [Fig. 2(b) and (d)]. Therefore, it might be part of a defence reaction. Although the investigation of the nature of these deposits was not the subject of the present study, the comparison to other works on Phytophthora infections [*4*, *16*] might indicate the presence of phenolic-like materials. Other cell wall appositions were found in the neighbourhood of hyphae between the cell wall and the plasmalemma [Fig. 2(a)]. These deposits were more or less electron-translucent with some dark inclusions. Compared to other investigations [*10*, *12*, *30*] callose might be involved in the formation of these structures.

Besides the investigations on the growth of *P. quercina* in oak roots, we tried to localize the peptide quercinin in infected tissue using immunofluorescence and immunogold cytochemical techniques. In these experiments, we used the primary antibody for cryptogein which was shown to pick up quercinin [*14*]. Previous work by Heiser *et al.* [*14*] has demonstrated that *P. quercina* synthesized quercinin in liquid culture and that quercinin was bound by antibodies raised against cryptogein on Western-blots. Five to seven days after infection, hyphae growing in the intercellular spaces of the cortical parenchyma were strongly highlighted by immunofluorescence staining [Fig. 3(a)]. Using a confocal laser scanning microscope, we demonstrated that only the cell wall of the pathogen was stained [Fig. 3(b)]. Furthermore, immunofluorescence suggested that quercinin was released into the invaded host cell [Fig. 3(b)]. Immunogold staining techniques in each of the four experiments verified the localization of the peptide along hyphal cell walls and its release into the apoplastic space [Fig. 4(c)] as well as into the cytoplasm of invaded cells [Fig. 4(d)]. We could show that invading hyphae were surrounded by a gelatinous matrix, as was observed by Coffey and Wilson [*4*] on haustoria of *Phytophthora infestans*. A comparable gelatinous matrix was not observed in healthy root tissue. Thus, this structure could either be part of a host defence reaction or built by the hyphae. Quercinin could be detected in relatively large amounts within this matrix [Fig. 4(d)]. Other hyphae present on Fig. 4(d) showed no labelling of cell walls. These hyphae possibly did not produce quercinin at the time of preparation. The *P. quercina* peptide was also found in the cell walls of mycelium samples. This fact shows that the secretion of quercinin by *P. quercina* is independent of the presence of a host plant, as could be supposed by results of previous investigations by Heiser *et al.* [*14*] demonstrating the secretion of quercinin in liquid culture.

The induction pattern of quercinin during the infection process followed the growth of the pathogen during the first 5 days after infection (Fig. 6). We do not yet know whether the interaction between *Q. robur* L. and *P. quercina* is of compatible or incompatible nature. The occurrence of defence reactions in response to infection observed in our cytological studies could indicate incompatibility. On the other hand, severe destruction of host root tissue could be observed, which is generally a characteristic for compatibility. Other investigations show that in potato [*20*] as well as in tobacco plants [*5*] infected either with *P. infestans* or with *P. parasitica*, the elicitin genes were down-regulated for the compatible but not for the incompatible interaction. If *P. quercina* is compatible to *Q. robur* L., these results differ from our observations.

As amino acid sequencing of quercinin has revealed a homology of 95 % to cryptogein (data not shown; unpublished work), we could speculate that the *P. quercina* elicitin could act in a way similar to cryptogein on the cellular level. Thus, quercinin which is set free in invaded tissue might interact locally with specific plasmalemma-bound receptors [*31*] inducing signal transduction and the production of reactive oxygen species such as superoxide and hydrogen peroxide as it was shown for the elicitin cryptogein [*25*, *28*]. Quercinin might also act as a sterol shuttle protein on plasmalemma membranes, as it was again demonstrated for cryptogein by Mikes *et al.* [*23*] and Vauthrin *et al.* [*31*]. This unique property of elicitins could contribute to the understanding of the role of quercinin in the host–pathogen interaction knowing that Phytophthora pathogens need sterols for vegetative growth and for the formation of sexual structures [*15*, *32*].

The systemic transport of Phytophthora elicitins in infected plants and within plants treated with these peptides was proven by the group of Devergne *et al.* [*9*]. The original report on the transport of *P. nicotianae* peptides causing severe wilt symptoms on tobacco plants was provided by Wolf and Wolf [*36*]. They localized the toxic agent in the xylem sap of infected tobacco plants. Recently, it was shown by Kang and Buchenauer [*22*] using immunocytochemical techniques that toxins of *Fusarium culmorum* were translocated upwards through the xylem vessels and phloem sieve tubes in infected wheat. Experiments are in progress to test whether quercinin stays in the root system of *P. quercina* infected oaks or whether it can spread systemically in the plant.

The authors wish to thank Prof. Dr Ricci and Dr Pernollet (Institut National de la Recherche Agronomique, France) for the cryptogein antibody. The skillful technical work on electron microscopy of Mrs Maria Wenzkowski is greatly appreciated. We also thank Prof. Dr Schleifer and Dr W. Ludwig (Mikrobiology, Technische Universität München) for the opportunity and their help to take laser scanning microscopy pictures. The project was financially supported by a DFG–grant No. OS 154/1–1.

REFERENCES

1. **Benhamou N, Côté F.** 1992. Ultrastructure and cytochemistry of pectin and cellulose degradation in tobacco roots infected by *Phytophthora parasitica* var. *nicotianae*. *Phytopathology* **82**: 468–478.
2. **Børja I, Sharma P, Krekling T, Lönneborg A.** 1995. Cytopathological response in roots of *Picea abies* seedlings infected with *Pythium dimorphum*. *Pytopathology* **85**: 495–501.
3. **Cahill D, Legge N, Grant B, Weste G.** 1989. Cellular and histological changes induced by *Phytophthora cinnamomi* in a group of plant species ranging from fully susceptible to fully resistant. *Phytopathology* **79**: 417–424.

4. **Coffey MD, Wilson UE.** 1995. Histology and cytology of infection and disease caused by *Phytophthora*. In: Erwin DC, Bartnicki-Garcia S, Tsao PH, eds. *Phytophthora its Biology, Taxonomy, Ecology and Pathology*. St. Paul, MN: APS Press, 289–301.
5. **Colas V, Conrod S, Venard P, Keller H, Ricci P, Panabieres F.** 2001. Elicitin genes expressed in vitro by certain tobacco isolates of *Phytophthora parasitica* are down regulated during compatible interactions. *Molecular Plant-Microbe Interactions* **14**: 326–335.
6. **Cooke D, Jung T, Naomi AW, Schubert R, Bahnweg G, Oßwald WF, Duncan J.** 1999. Molecular evidence supports *Phytophthora quercina* as a new species. *Mycological Research* **103**: 799–804.
7. **Csinos A, Hendrix JW.** 1977. Toxin produced by *Phytophthora cryptogea* active on excised tobacco leaves. *Canadian Journal of Botany* **55**: 1156–1162.
8. **Dawson P, Weste G.** 1984. Impact of root infection by *Phytophthora cinnamomi* on the water relations of two Eucalyptus species that differ in susceptibility. *Phytopathology* **74**: 486–490.
9. **Devergne J-C, Bonnet Ph, Panabières F, Blein J-P, Ricci P.** 1992. Migration of the fungal protein cryptogein within tobacco plants. *Plant Physiology* **99**: 843–847.
10. **Enkerli K, Hahn MG, Mims CW.** 1997. Ultrastructure of compatible and incompatible interactions of soybean roots infected with the plant pathogenic oomycete *Phytophthora sojae*. *Canadian Journal of Botany* **75**: 1493–1508.
11. **Erwin D, Ribeiro O.** 1996. *Phytophthora Diseases Worldwide*. St. Paul, MN: APS Press.
12. **Hanchey P, Wheeler H.** 1971. Pathological changes in ultrastructure: tobacco roots infected with *Phytophthora parasitica* var. *nicotianae*. *Phytopathology* **61**: 33–39.
13. **Hansen E, Delatour C.** 1999. Phytophthora species in oak forests of north-east France. *Annales Des Sciences Forestiere* **56**: 539–547.
14. **Heiser I, Fromm J, Giefing M, Koehl J, Jung T Oßwald W.** 1999. Investigations on the action of *Phytophthora quercina*, *P. citricola* and *P. gonapodyides* toxins on tobacco plants. *Plant Physiology and Biochemistry* **37**: 73–81.
15. **Hendrix JW.** 1970. Sterols in growth and reproduction of fungi. *Annual Review of Phytopathology* **8**: 111–130.
16. **Jang JC, Tainter FH.** 1990. Cellular responses of pine callus to infection by *Phytophthora cinnamomi*. *Phytopathology* **80**: 1347–1352.
17. **Jung T, Blaschke H, Neumann P.** 1996. Isolation, identification and pathogenicity of *Phytophthora* species from declining oak stands. *European Journal of Forest Pathology* **26**: 253–272.
18. **Jung T, Blaschke H, Oßwald WF.** 2000. Involvement of soil-borne *Phytophthora* species in Central European oak decline and the influence of site factors on the disease. *Plant Pathology* **49**: 706–718.
19. **Jung T, Cooke D, Blaschke H, Duncan J, Oßwald WF.** 1999. *Phytophthora quercina* sp. nov, a new species causing root rot on European oak species. *Mycological Research* **103**: 785–798.
20. **Kamoun S, van West P, Jong A, Groot K, Vleeshouwers A, Govers F.** 1997. A gene encoding a protein elicitor of *Phytophthora infestans* is down-regulated during infection of potato. *Molecular Plant-Microbe Interactions* **1**: 13–20.
21. **Kamoun S, Young M, Förster H, Coffey MD, Tyler BM.** 1994. Potential role of elicitins in the interaction between *Phytophthora* species and tobacco. *Applied and Environmental Microbiology* **1994**: 1593–1598.
22. **Kang Z, Buchenauer H.** 1999. Immunocytochemical localization of fusarium toxins in infected wheat spikes by Fusarium culmorum. *Physiological and Molecular Plant Pathology* **55**: 275–288.
23. **Mikes V, Milat M-L, Ponchet M, Ricci P, Blein J-P.** 1997. The fungal elicitor cryptogein is a sterol carrier protein. *FEBS Letters* **416**: 190–192.
24. **Ploetz RC, Schaffer B.** 1989. Effects of flooding and *Phytophthora* root rot on net gas exchange and growth of avocado. *Phytopathology* **79**: 204–208.
25. **Pugin A, Guern J.** 1996. Mode of action of elicitors: involvement of plasma membrane functions. *Comptes Rendus de l' Académie des Sciences (Paris), Sciences de la Vie* **319**: 1055–1061.
26. **Spurr AE.** 1969. A low-viscosity epoxy resin embedding medium for electron microscopy. *Journal of Ultrastructure Research* **26**: 31–41.
27. **Sterne RE, Kaufmann MR, Zentmyer GA.** 1978. Effect of *Phytophthora* root rot on water relations of avocado: Interpretation with a water transport model. *Phytopathology* **68**: 595–602.
28. **Tavernier E, Wendehenne D, Blein JP, Pugin A.** 1995. Involvement of free calcium in action of cryptogein, a proteinaceous elicitor of hypersensitve reaction in tobacco cells. *Plant Physiology* **109**: 1025–1031.
29. **Tippet JT, O'Brien TP, Holland AA.** 1977. Ultrastructural changes in eucalypt roots caused by *Phytopthora cinnamomi*. *Physiological Plant Pathology* **11**: 279–286.
30. **Trillas MI, Cotxarrera L, Casanova E, Cortadellas N.** 2000. Ultrastructural changes and localization of chitin and callose in compatible and incompatible interactions between carnation callus and *Fusarium oxysporum*. *Physiological and Molecular Plant Pathology* **56**: 107–116.
31. **Vauthrin S, Mikes V, Milat M-L, Ponchet M, Maume B, Osman H, Blein J-P.** 1999. Elicitins trap and transfer sterols from micelles, liposomes and plasma membranes. Biochemica. *Biophysica Acta* **1419**: 335–432.
32. **Weete JD.** 1989. Structure and function of sterols in fungi. *Advances in Lipid Research* **23**: 115–165.
33. **Wendehenne D, Binet MN, Blein JP, Ricci P, Pugin A.** 1995. Evidence for specific, high affinity binding sites for a proteinaceous elicitor in tobacco plasma membrane. *FEBS Letters* **374**: 203–207.
34. **Widmer TL, Graham JH, Mitchell DJ.** 1998. Histological comparison of fibrous root infection of disease-tolerant and susceptible citrus hosts by *Phytophthora nicotianae* and *P. palmivora*. *Phytopathology* **88**: 389–395.
35. **Wolf FT.** 1933. The pathology of tobacco black shank. *Phytopathology* **23**: 605–612.
36. **Wolf FT, Wolf FA.** 1954. Toxicity as a factor in Tobacco black shank. *Journal of the Mitchell Society* **70**: 244–255.
37. **Yu LM.** 1995. Elicitins from *Phytophthora* and basic resistance to tobacco. *Proceedings of the National Academy of Sciences of the U.S.A.* **92**: 4088–4094.